



High pressure anode operation of direct methanol fuel cells for carbon dioxide management

Michael D. Lundin¹, Mark J. McCreehy*

Department of Chemical & Biomolecular Engineering, University of Notre Dame du lac, 181 Fitzpatrick Hall, Notre Dame, IN 46556, United States

ARTICLE INFO

Article history:

Received 28 August 2010
Received in revised form 13 October 2010
Accepted 14 October 2010
Available online 10 March 2011

Keywords:

DMFC
Pressure
Carbon dioxide (CO₂)
Bubbles
Vacuum

ABSTRACT

Experiments with independent pressurization of the direct methanol fuel cell anode and cathode allow for the observation of DMFC operation with carbon dioxide gas formation suppressed. Results indicate that the limiting current density is strongly related to the applied pressure, and, therefore, to the presence of CO₂ in the liquid phase. An additional experiment where CO₂ is allowed to accumulate in recycled anode fuel solution over a period of time and is then stripped from solution using nitrogen gas indicates that the presence of CO₂ in anode fuel solution at any pressure contributes to significant decreases in power and current density. Because CO₂ bubbles are ubiquitous in direct methanol fuel cells, this finding is key to the optimization of these systems.

© 2010 Elsevier B.V. All rights reserved.

1. Introduction

The fuel cell is attractive for the conversion of chemical energy into electrical energy due to high efficiencies and low emissions. While H₂ powered cells have numerous potential applications, the need to power portable devices is driving development of fuel cells with liquid fuels.

At 3800 kcal l⁻¹, liquid methanol has a higher energy density than hydrogen at 360 atm (658 kcal l⁻¹) [1] and other gas fuels and is more easily processed and stored. The direct methanol fuel cell (DMFC) takes advantage of these properties and is a potential power source for portable applications; however, its current shortcomings in kinetics and methanol crossover problems yield a power density nearly an order of magnitude lower than that of a hydrogen fueled PEMFC [2]. Because of those limitations, every opportunity to optimize cell operation must be considered.

To ensure maximum current density and optimal reaction conditions, efficient removal of both CO₂ from the anode surface and water from the cathode surface is essential. While water management at the cathode has been studied [3] due to its occurrence in H₂ PEM cells, removal of CO₂ at the anode has been largely overlooked

and remains an important issue for research in the development of DMFCs.

The topic of CO₂ gas evolution in DMFCs has received some attention in the literature. Gas bubble growth and release from the diffusion layer was investigated by Mench et al. [4]. Argyropoulos et al. [5] witnessed the blocking of parallel flow channels at low flow rates and high current densities while studying the CO₂ flow characteristics visually in situ. Yang et al. [6] conducted a comprehensive investigation into effects of flow field designs and cell orientation while qualitatively studying CO₂ bubble behavior using visualization in situ. While Yang et al. did not encounter the channel blocking slugs that Argyropoulos encountered, they did show that the presence of large gas slugs in the flow field correlated to decreased cell performance. Lundin and McCreehy [7] investigated and modeled the impact that the CO₂ solubility of the anode fuel solution has on the evolution of CO₂ gas and explored methods of enhancing CO₂ solubility through the addition of various chemicals.

In the typical DMFC, methanol in a low concentration (1 M) solution is fed to the anode flow field and contacts the anode catalyst via the diffusion layer while the CO₂ being produced traverses the diffusion layer to the anode flow field in reverse. The quantity of CO₂ being produced is directly related to current produced by the cell. The fuel for the reaction is liquid water and methanol, so the CO₂ produced at the anode is initially in the liquid phase. Because of the large quantities of CO₂ that evolve, the liquid fuel quickly becomes saturated and gas phase CO₂ forms. This gas formation, under poorly optimized operating conditions, may consume a significant fraction of the flow field volume. Carbon dioxide gas limits

* Corresponding author. Tel.: +1 574 631 7146; fax: +1 574 631 8366.

E-mail addresses: mlundin@alumni.nd.edu (M.D. Lundin), mjm@nd.edu (M.J. McCreehy).

¹ Current address: Center for Environmentally Beneficial Catalysis, University of Kansas, 1501 Wakarusa Dr., Lawrence, KS 66047, United States.

mass transfer of methanol and water to the anode catalyst surface. The presence of gas indicates that the fuel solution is saturated with CO_2 and that diffusion of CO_2 from the catalyst surface may be limited. Initiation of two-phase flow leads to a capillary bubble train in the flow field creating pressure drops that decrease the efficiency of a stack by both increasing pumping power requirements and methanol crossover. In portable systems the problem of fuel supply is generally overcome by increasing the flow-rate of the anode fuel, which can have the undesirable side effects of further increasing methanol crossover and creating temperature gradients if the fuel solution is not properly preheated. Unfortunately, the formation of capillary bubble trains at high current production is inevitable even under these conditions.

The true impact of carbon dioxide gas formation on the performance of a direct methanol fuel cell remains unknown due to the difficulty in creating an environment where carbon dioxide gas is not present but normal cell operation is still possible. One technique to suppress the formation of carbon dioxide gas is to operate the cell at high pressure. Carbon dioxide, while only slightly soluble in water or water/methanol mixtures at atmospheric pressure, becomes increasingly soluble at high pressures. Cell operation at pressures sufficient to elevate the carbon dioxide solubility of fuel solution beyond the carbon dioxide production capacity of the cell enable cell operation where the anode flow-field is 100% liquid.

A thorough review of the literature indicates that high pressure operation of the anode has not been considered or attempted. The following is a comprehensive investigation into the effect of pressure on both the anode and the cathode independently for the purpose of investigating the benefits and consequences of eliminating multiphase flows in direct methanol fuel cells.

2. Experimental methods

2.1. Hardware setup

The fuel cell hardware used for the experiments consisted of a single cell provided by Fuel Cell Technologies, Inc. capable of utilizing a 5 cm^2 membrane electrode assembly. The cell consisted of a pair of POCO™ graphite blocks with a precision machined single serpentine flow-pattern. The graphite blocks also acted as preliminary current collectors which were in direct contact with the gas diffusion layers of the membrane electrode assembly. Gold plates sandwiched in between the graphite plates and aluminum end plates provided a mechanism by which to attach the test load and electrical monitoring hardware. Membrane electrode assemblies (MEAs) were provided by FuelCellStore.com. Each MEA had an active area of 5 cm^2 with an anode catalyst loading of $4.0\text{ mg Pt-Ru cm}^{-2}$, a cathode loading of 2.0 mg Pt cm^{-2} , a Nafion-117 polymer electrolyte separating the anode and cathode. The gas diffusion layers at the anode and cathode were carbon cloth and ETEK ELAT®, respectively.

Each aluminum end plate contained an electric resistance heater and thermocouple for temperature control. Liquid feed to the anode was produced by a “GA series” gear pump provided by Micropump with steady flow-rates available in the range of $0.01\text{--}50\text{ cm}^3\text{ min}^{-1}$. Gas feed to the cathode was provided by high pressure gas cylinders controlled by an MKS mass flow controller with flow rates available up to 500 scc min^{-1} . Measurements of the cell’s electrical characteristics were provided by a commercially available test load, provided by Scribner Associates as a model 890CL. The liquid pump, the mass flow controller, the heaters, and the test load were controlled by a computer running Scribner’s proprietary FuelCell software (Version 3.4d). Preheating of the liquid feed was accomplished through electrical heating of the tubing and pump head controlled by a stand alone Omega CN76000 controller.

The anode and cathode were adapted in-house to be capable of pressurization. Tubing between the mass flow controller and the cathode was replaced with 316 stainless steel tubing. Gas exiting the cathode was run through a liquid trap prior to exiting the system via a back pressure regulator provided by Tescom. The liquid solution for anode feed was contained in a recycle loop made entirely of 316 stainless steel components to allow for the required pressurization and prevent component corrosion. Liquid, contained in a feed tank, was fed to the anode via the gear pump. Upon exiting the anode, the liquid and any gas produced by the reaction was returned to the feed tank where the gas and liquid was separated. The feed tank was simultaneously purged with nitrogen gas provided by a high pressure cylinder. Purge gas and reaction produced carbon dioxide gas exited the system via a second back pressure regulator. The result of the setup was that the entire anode feed loop could be pressurized under a nitrogen gas pad, with the pressure on the cathode feed independently adjustable. Pressure gauges for each side were present for pressure monitoring as well as a differential pressure gauge between the anode and cathode to ensure that the pressure gradient across the MEA could be closely monitored and controlled. The alternative vacuum setup was one where the nitrogen purge line was replaced with a vacuum pump, and the back pressure regulator valved off, and a vacuum gauge installed in place of the normal pressure gauge on the anode side. Vacuum was not applied to the cathode. A schematic is provided in Fig. 1.

2.2. Operating conditions

A valid comparison of cell operation at different operating parameters requires three things to be compared: the highest voltage at which current may be drawn (the onset voltage), the maximum power density, and the maximum current density. All of these three metrics are obtainable from a voltage scan, which is the standard test used for these experiments.

Because of the many adjustable parameters, the only standard operating conditions were that all experiments were conducted at 70°C , the feed preheated to 60°C and with the cathode feed consisting of pure extra dry oxygen gas made available from high pressure cylinders. Typical conditions involved the cathode feed being delivered to the cell at 150 scc min^{-1} . The typical anode feed consisted of a methanol/water solution where the concentration of methanol was 1 M, achieved by adding 960 ml of DI water to 40 ml of HPLC grade methanol, and delivered to the cell at a flow-rate of 5 ml min^{-1} . When the cell was operated with the anode fuel supply under pressure, the cathode was typically pressurized to 5 psi above that of the anode to prevent enhancement of methanol crossover. Because of this, each experiment generally included at least one voltage scan where both the anode and cathode were operated at 0 psig, and at least one voltage scan where the anode was operated at 0 psig and the cathode was operated at 5 psig.

3. Results and discussion

3.1. Initial observations with pressure increases

With no data available in the literature regarding the anode pressurization in direct methanol fuel cells, the initial experiments were a simple series of voltage scans having the primary objective of testing the stability of the system with the pressure modifications and the secondary objective of investigating whether the system would react at all to increases in pressure.

Each voltage scan was run at 70°C with the anode feed preheated to 60°C . The 1 M methanol/water solution was fed to the anode at a flow-rate of 5 ml min^{-1} and was pressurized under a nitrogen gas pad. Extra dry oxygen was fed to the cathode at

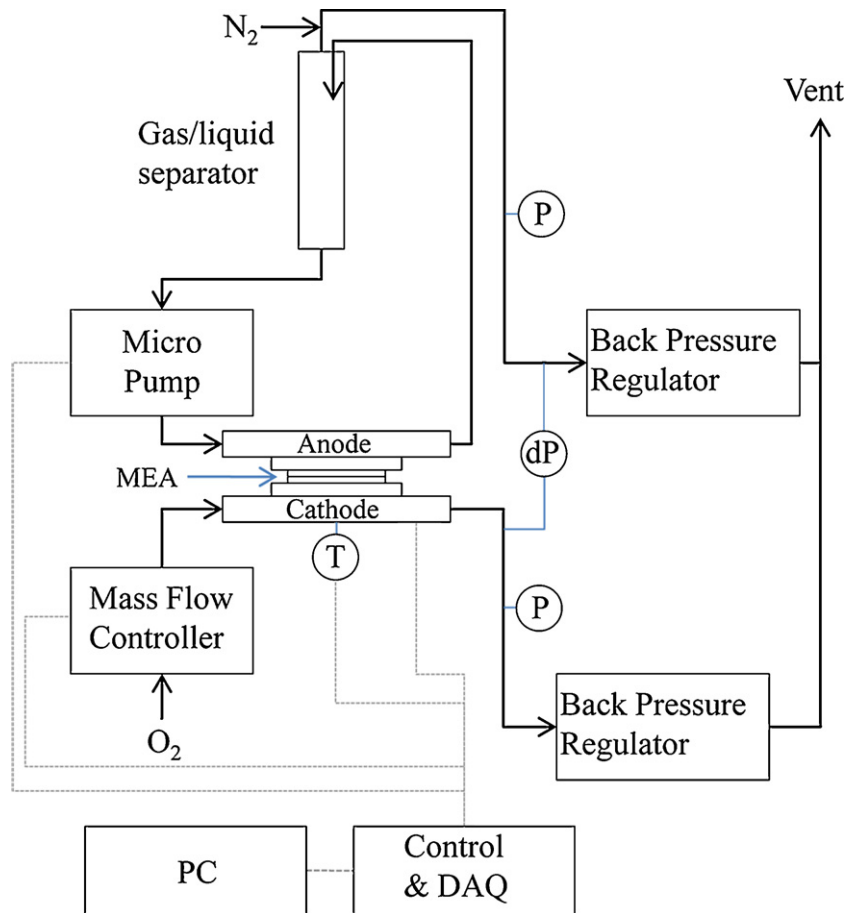


Fig. 1. Schematic diagram of DMFC testing system with modifications for operation at high pressure.

150 scc min⁻¹. Voltage scans were conducted with the anode at 0, 25, 50, and 75 psig. Pressure was applied to the cathode in each experiment – with the exception of the atmospheric scan – such that the cathode operated at a pressure 5 psi above that of the anode. Results are shown in Fig. 2.

The primary objective was satisfied with no detectable leaks or instabilities at pressures as high as 75 psig. Results of the secondary objective were inconclusive. It was anticipated that increasing the solubility of carbon dioxide gas via increases in operating pressure

would have the greatest effect at the end of the voltage scan, seen as an increase in the limiting current density. Improved mass transfer of methanol to the catalyst surface due to a decrease in void space from carbon dioxide gas was anticipated. The voltage scans indicate a mass transfer limitation occurring immediately after the peak power density is reached, and well before the limiting current density present at atmospheric pressure.

Because the atmospheric test did not include a pressure gradient across the MEA, the results of the high pressure experiments are not directly comparable to the atmospheric test. Based solely on these results, the lack of comparable data at atmospheric pressure makes it difficult to determine whether the source of the increase in peak power density resulted from the pressure increase, or the presence of a pressure gradient. The fact that the peak power density does not appear to depend on the amount of pressure indicates that it is a result of the pressure gradient. Further tests needed to be conducted to determine source of the mass-transfer limitation, as well as to explore the effects of pressure under different operating conditions.

3.2. High methanol concentration at high pressure

A second series of experiments was conducted with a 2 M methanol concentration in the anode feed for the purposes of determining the source of the apparent mass transfer limitation experienced when pressure is applied to the anode.

Each voltage scan was run at 70 °C with the anode feed pre-heated to 60 °C. The methanol/water solution was fed to the anode at a flow-rate of 5 ml min⁻¹ and was pressurized under a nitrogen gas pad. Extra dry oxygen was fed to the cathode at 150 scc min⁻¹.

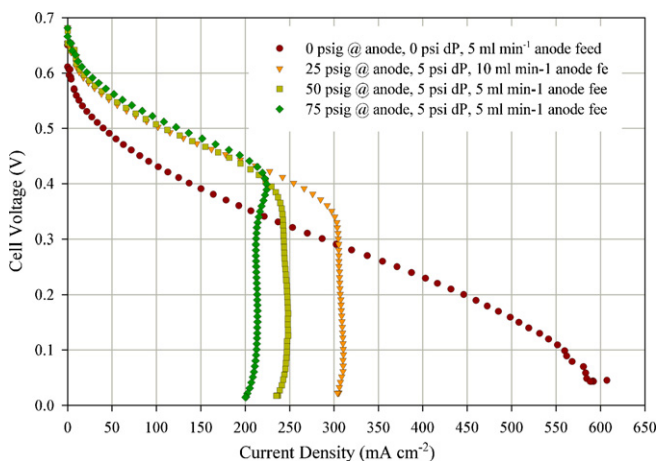


Fig. 2. Results of initial experiments conducted at high pressure. All experiments conducted at 70 °C with a cathode flow-rate of 150 scc min⁻¹, and an anode fuel consisting of 1 M methanol in water. dP is (cathode–anode).

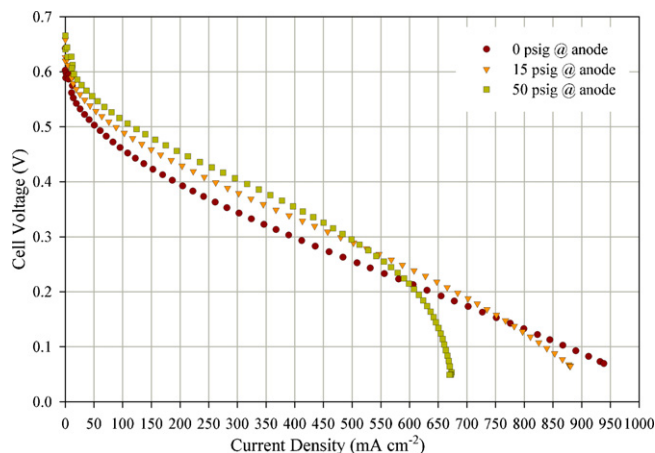


Fig. 3. Selected results of experiments highlighting the effect of pressure when the methanol concentration in the anode fuel is 2 M. All experiments conducted at 70 °C with an anode flow-rate of 5 ml min⁻¹ and a cathode flow-rate of 150 scc min⁻¹.

Pressure was applied to the cathode in each experiment (as appropriate), such that the cathode operated at a pressure 5 psi above that of the anode.

Fig. 3 highlights the effect of pressure with 2 M methanol solution and, though it is not nearly as severe with the 2 M methanol solution compared to the 1 M methanol preliminary experiments, it is apparent that a mass-transfer limitation at high pressures still appears, decreasing the maximum current density as pressure is increased.

Concerning the question of peak power density, in this experiment, all three voltage scans involved a pressure gradient of 5 psi (cathode–anode). Despite the pressure gradient, the peak power appears to increase substantially at high pressure versus atmospheric pressure, though the effect appears to be limited to an initial jump when pressure is applied, and remains constant afterward.

Fig. 4 highlights the effect of the anode and cathode flow-rates on the polarization curve. Increasing the cathode flow-rate by a factor of four results in no change in either the peak power density or the limiting current density, while doubling and tripling the anode flow-rate result in incrementally higher limiting current densities and peak power densities.

That the limiting current density and peak power density are sensitive to changes in anode flow-rate and that they are insen-

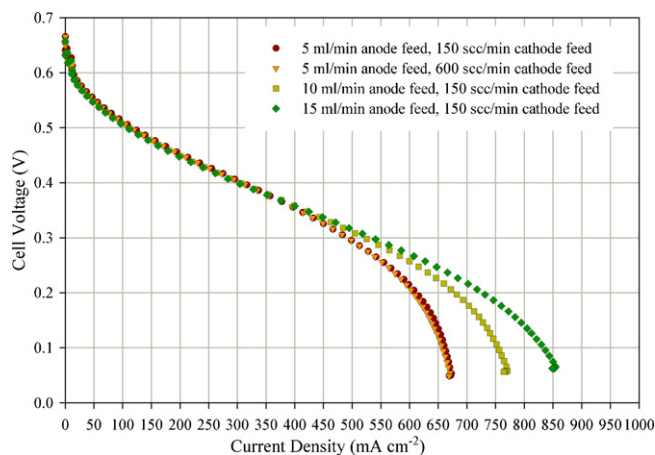


Fig. 4. Selected results of experiments highlighting the effect of changing anode and cathode flow-rates. All experiments conducted at 70 °C with an anode fuel consisting of 2 M methanol in water, an anode pressure of 50 psig, and a cathode pressure of 55 psig.

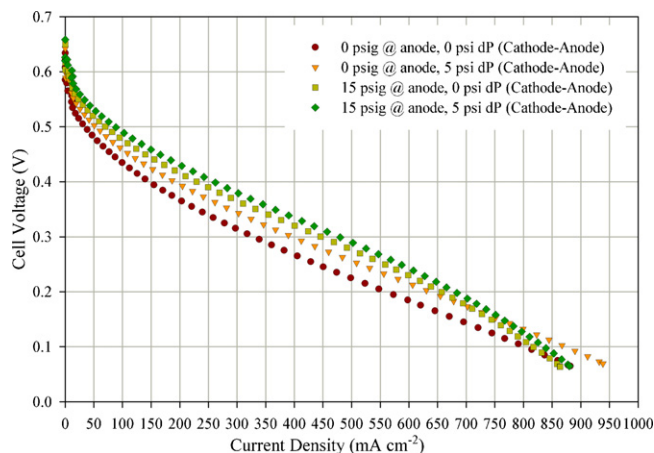


Fig. 5. Selected results of experiments highlighting the effect of pressure gradient across the membrane at high and low total pressure. All experiments conducted at 70 °C with an anode flow-rate of 5 ml min⁻¹, a cathode flow-rate of 150 scc min⁻¹, and an anode fuel consisting of 2 M methanol in water.

sitive to changes in cathode flow-rate indicate that the source of the apparent mass-transfer limitation occurs on the anode side of the cell. This is supported by the combined results of Figs. 3 and 4, where the limiting current density has an approximately linear correlation to the methanol concentration. A fact further supported by the results of Schonewill [8], who asserts that the concentration gradient limited mass-transfer of methanol to the catalyst surface is the sole source of mass-transfer limitations in DMFCs.

High anode pressures eliminate the formation of carbon dioxide gas, and the binary diffusion coefficient of liquids is independent of pressure [9]. This would seem to eliminate the possibility that increases in pressure affect the diffusion of methanol to the catalyst surface, which leads to the possibility that carbon dioxide plays a role in the mass-transfer limitation.

A final comparison of results in the 2 M methanol experiments involved the application of differential pressure across the membrane electrode assembly. Fig. 5 illustrates the results of a 5 psi difference between the cathode and anode at 0 psig anode pressure and 15 psig anode pressure versus those of equally pressurized sides. In both cases, the application of differential pressure results in a general performance enhancement, with increases in both peak power density and limiting current density. The change in curve shape from the application of pressure to the anode is still notable, similar to that of previous experiments.

3.3. Investigation into the presence of hysteresis

A series of experiments were conducted to test for the presence of hysteresis after pressure operation. Each voltage scan was run at 70 °C with the anode feed preheated to 60 °C. The 1 M methanol/water solution was fed to the anode at a flow-rate of 5 ml min⁻¹ and was pressurized under a nitrogen gas pad. Extra dry oxygen was fed to the cathode at 150 scc min⁻¹. Pressure was applied to the cathode in each experiment (as appropriate), such that the cathode operated at a pressure 5 psi above that of the anode. Voltage scans were conducted in the order listed in Fig. 6, starting at 0 psig at the anode, ramping up to 50 psig, and back down to 0 psig.

Fig. 6 shows that there is no detectable hysteresis after pressurization of the cell to 50 psig. This is an important result because it indicates that the phenomena generating the apparent mass-transfer limitations at high pressures is not a result of pressure adversely affecting cell components. If, for example, the pressure applied to the cell was compressing the membrane or gas diffusion

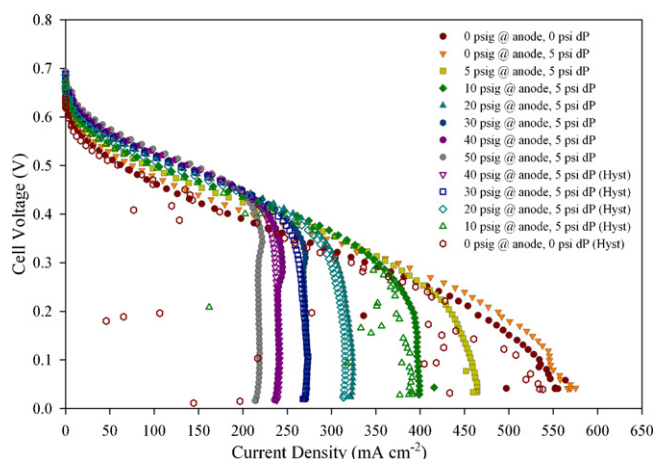


Fig. 6. Results of experiments conducted to test for hysteresis in the application of pressure. All experiments conducted at 70 °C with an anode flow-rate of 5 ml min⁻¹, a cathode flow-rate of 150 scc min⁻¹, and an anode fuel consisting of 1 M methanol in water. dP is (cathode–anode).

layers, it is highly probable that some degree of elastic hysteresis would occur and be observed in the experiment. That no hysteresis occurs is a good indication that the observed effects of pressure result from pressure effects on mass transfer or reaction mechanism.

The results of this experiment also underscore the highly repeatable nature of the pressure effect. Universally, for a given flow-rate and methanol concentration, the application of a given amount of pressure always results in the same limiting current density. This is further investigated in Section 3.5.

That the results of the return scans show high levels of instability at low pressure are not evidence of hysteresis, but artifacts of carbon dioxide saturation in the recycled anode fuel. Due to difficulties in exactly replicating cell performance between fuel solutions, the same fuel solution was used for the entire experiment. When the cell was operated at pressures up to 50 psig, carbon dioxide from the anode reaction was allowed to concentrate in the fuel solution to levels above the saturation limit at low pressures. Carbon dioxide gas formed as the low pressure fuel entered the heated cell. The presence of large amounts of carbon dioxide gas in the anode flow field during the voltage scan led to the instabilities observed in Fig. 6.

3.4. Observations during vacuum operation

Because the application of pressure leads to substantial decreases in cell performance, it is logical to consider what happens when the anode is operated at sub-atmospheric pressure. Fig. 7 displays the results of a series of voltage scans conducted under vacuum pressure at 70 °C (the anode feed was not preheated in order to prevent premature gas formation in the feed lines). The 1 M methanol/water solution was fed to the anode at a flow-rate of 5 ml min⁻¹ and extra dry oxygen was fed to the cathode at 150 scc min⁻¹.

A change to the hardware setup was required to make this experiment possible: a vacuum pump was connected to the port where nitrogen gas had previously been provided for pressurization, the pressure gauge was replaced with a vacuum pressure gauge, and the original exit line to vent was sealed off. Vacuum was applied until electrical equilibrium was achieved prior to starting each voltage scan.

Results of the experiment indicate that the application of vacuum to the anode fuel loop does enhance performance and that the performance enhancement is different from that gained by the

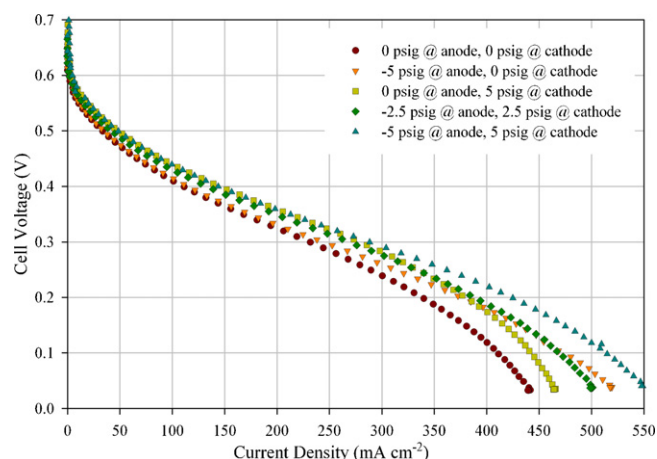


Fig. 7. Results of an experiment conducted to investigate effects of vacuum pressure. All scans conducted at 70 °C with an anode flow-rate of 5 ml min⁻¹, a cathode flow-rate of 150 scc min⁻¹, and an anode fuel consisting of 1 M methanol in water.

application of pressure to the cathode. The application of 5 psig vacuum to the anode results in a significantly higher limiting current density than the application of 5 psig pressure to the cathode resulting in an equivalent differential pressure across the MEA. At the same time, the application of pressure to the cathode results in a higher peak power density than the application of vacuum to the anode. The application of 2.5 psig vacuum to the anode and 2.5 psig pressure to the cathode results in approximately the benefits of both individual effects. All of these facts combined indicate that the benefits realized from the application of vacuum to the anode loop are inherently different and independent from those resulting out of pressure increases to the cathode. They also suggest that the benefits from the application of differential pressure across the membrane electrode assembly may be optimized by adjusting the manner in which the differential pressure is applied.

3.5. The relationship between pressure and limiting current density

An analysis to determine the relationship between pressure and limiting current density was conducted. Data collected from several experiments were used in the analysis. For comparison purposes, selected scans were conducted at 70 °C with an anode flow-rate of 5 ml min⁻¹, a cathode flow-rate of 150 scc min⁻¹, a differential pressure of 5 psi (cathode–anode), and the feed preheated to 60 °C. 120 psig at the anode was the pressure limit of the system due to the design of the tank cylinder regulators, so data beyond that were not available. All available data for each methanol concentration are displayed if the conditions for the experiment in which it was conducted matched those described.

The collected data are illustrated in Fig. 8. A dashed line indicating the theoretical limit of carbon dioxide solubility in the anode fuel solution as calculated from the model with interpolated data from Carroll et al. [11]. The area to the left of the dashed line is the region where gas formation is expected, the area to the right of the dashed line is the region where the solubility of the fuel solution is sufficient for CO₂ to stay in solution as a liquid. Inspection of the data indicate that the limiting current of the cell is related to the operating pressure. It may also be observed that the application of pressure has a diminishing effect, ending after carbon dioxide gas formation is suppressed. The effect appears to plateau shortly after the limit of carbon dioxide is reached, likely because gas formation continues to occur in areas of locally high carbon dioxide concentration that are not predicted by the models for the bulk solution. The relationship between limiting current density and

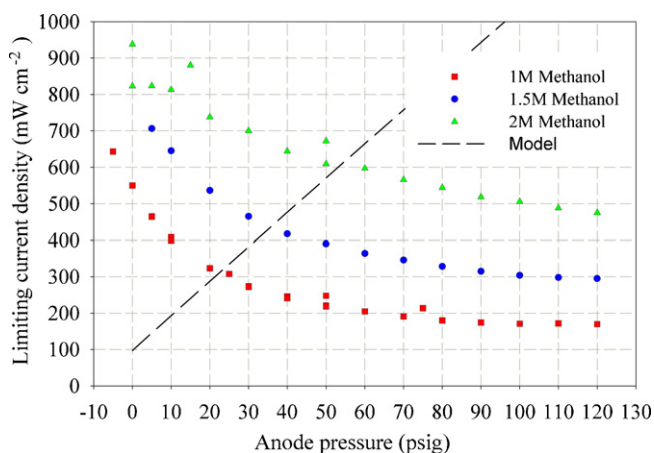


Fig. 8. The relationship between pressure and limiting current density, with theoretical limit of CO_2 solubility illustrated. Each scan conducted at 70°C with an anode flow-rate of 5 ml min^{-1} , a cathode flow-rate of 150 scc min^{-1} , and a differential pressure of 5 psi (cathode–anode).

anode pressure is further evidenced that carbon dioxide plays some significant role in the mass transfer limitation experienced at the anode, since the only real effect of pressure is to further dissolve carbon dioxide.

The relationship between the limiting current density and the system pressure suggests that the desorption of CO_2 from the catalyst surface may be more influential in limiting the reaction rate than previously considered. Before additional methanol can chemisorb onto the catalyst surface, carbon dioxide must desorb. If the desorption of carbon dioxide from the catalyst surface is limited by its ability to diffuse into the bulk solution, it may act as a significant contributor to the rate limitation. This is supported by the work of Bellows et al. [10].

Using data from Ref. [11] to convert the system pressure to carbon dioxide solubility and the limiting current density as an expression of the effective reaction rate, Fig. 9 shows that the relationship between the reaction rate and the inverse of CO_2 solubility. Assuming Langmuir–Hinshelwood kinetics, a linear relationship implies that the reaction order with respect to CO_2 concentration is -1 . The plot is imperfect in that it uses CO_2 solubility in place of CO_2 concentration, which is incorrect as the solubility exceeds the CO_2 production capacity of the cell. At least initially, when the CO_2 solubility is likely to closely match the CO_2 concentration, the plots appear to be linear.

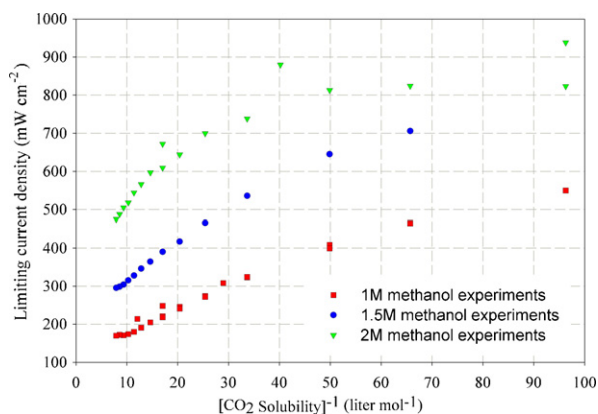


Fig. 9. The relationship between limiting current density and the inverse of CO_2 solubility. Scans conducted at 70°C with an anode flow-rate of 5 ml min^{-1} , a cathode flow-rate of 150 scc min^{-1} , and a differential pressure of 5 psi (cathode–anode).

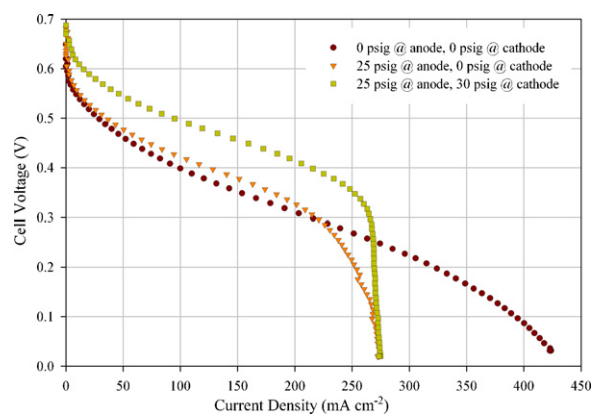


Fig. 10. Results of investigation into cell behavior when anode pressure is not compensated for at the cathode. All scans conducted at 70°C with an anode flow-rate of 5 ml min^{-1} , a cathode flow-rate of 150 scc min^{-1} , and an anode fuel consisting of 1 M methanol in water.

3.6. Observations with anode at high pressure

All data acquired with the anode under pressure or vacuum have been with the cathode pressure either at a pressure matching or 5 psi above that of the anode specifically to avoid the enhancement of methanol crossover due to a pressure gradient. The final question, then, is what happens if the anode is operated at pressures significantly above that of the cathode? An experiment was conducted at 70°C with an anode flow-rate of 5 ml min^{-1} , a cathode flow-rate of 150 scc min^{-1} , and an anode fuel consisting of 1 M methanol in water. The first scan was conducted with both the anode and the cathode at 0 psig. A second scan was conducted with the anode at 25 psig and the cathode at 0 psig, and a third scan was conducted with the anode at 25 psig and the cathode at 30 psig.

Results of the experiment are shown in Fig. 10. The results of pure atmospheric operation are typical for the conditions. Increasing the anode pressure to 25 psig allows the power density to initially exceed that of the pure atmospheric scan, eventually reaching a similar peak power density, but then experiencing a rapid decline in current density typical of the mass-transfer effects seen in previous high pressure experiments. Increasing the cathode pressure to 30 psig while maintaining the anode at 25 psig increases the initial and peak power density, but results in an identical limiting current density of 275 mA cm^{-2} to that of the second scan. This result leads to the conclusion that the pressure related current density limitation is independent of the differential pressure across the membrane electrode assembly.

Due to the nature of the setup and the design of the circulation loop required to operate at high pressures, direct, quantitative, measurements of gas/bubble formation was not possible. However, with a clear section of tubing installed at the anode discharge, visual observation indicated qualitatively that gas formation decreased rapidly as pressure increased. At the highest operating pressures, virtually no gas was formed.

3.7. The effects of CO_2 accumulation in anode fuel supply

Questions regarding the role of carbon dioxide at the DMFC arising out of the suppression of gas formation require further investigation into the significance of the problem, particularly at atmospheric pressures where DMFCs are typically operated. An investigation into the effect of carbon dioxide accumulation in a recycled anode fuel supply was conducted to determine the extent of its influence at atmospheric pressure. The experiment involved running voltage scans every 15 min for 51 h before sparging the

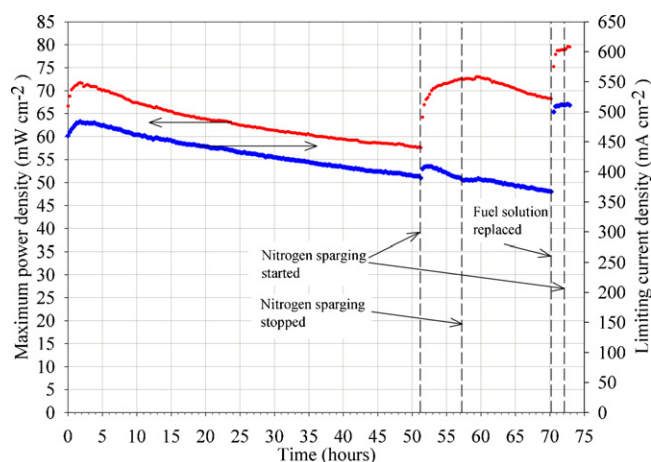


Fig. 11. Results of a time study analyzing the effect of carbon dioxide accumulation in recycled anode fuel and the effects of carbon dioxide removal by stripping with nitrogen gas. Each point represents the results of a full voltage scan conducted at 70 °C with an anode flow-rate of 5 ml min⁻¹, a cathode flow-rate of 150 scc min⁻¹, and anode fuel consisting of 1 M methanol in water.

anode fuel with nitrogen gas in an attempt to strip CO₂ gas from the fuel. Voltage scans continued to run every 15 min during the sparging. After 6 h, the sparging was halted and the voltage scans allowed to continue every 15 min. After an additional 13 h, the fuel was replaced with a fresh solution with voltage scans continuing every 15 min for the next 2 h before nitrogen sparging was started again. Voltage scans were conducted at 70 °C with the feed pre-heated to 60 °C. The anode flow-rate was a constant 5 ml min⁻¹ and the cathode flow-rate was a constant 150 scc min⁻¹. No pressure was applied to either side and the anode fuel was a solution of 1 M methanol in water.

The results of the experiment are displayed in Fig. 11, with the limiting current density and maximum power density individually tracked. Both measurements peaked shortly after the experiment began, indicating the typical break-in period for a new membrane electrode assembly. After the initial peak, a steady decline in performance is observed until the introduction of nitrogen gas. Immediately after the nitrogen gas is started, a large jump in the limiting current density is observed, eventually resulting in performance equaling that of the post break-in peak. The maximum power density also experiences a small jump, but resumes its decline before the nitrogen sparging is stopped and before it returns to the post break-in peak.

After nitrogen sparging is halted, both limiting current density and maximum power density remain stable for approximately 2 h before resuming their decline. Once the fuel solution is replaced with a freshly made solution, both limiting current density and maximum power density jump to levels above that of the original post break-in peak. After nitrogen sparging was reintroduced approximately 2 h later, no significant change was observed.

A reasonable interpretation of these results is that the nitrogen gas removed carbon dioxide from solution, allowing the limiting current density to fully recover. The peak power density was unable to recover because its decline was primarily due to a corresponding decline in the concentration of methanol in the anode fuel. Both the limiting current density and peak power density remained stable after nitrogen sparging was stopped because it took several hours for all of the fuel in the 1 l tank to be exposed to the reaction, after which the decline is again observed.

With the replacement of fuel, both the concentrations of carbon dioxide and that of methanol are reset to the original values, so both the limiting current density and the peak power density improve to above post break-in levels. The difference cannot be accounted

for, however it is not unusual that DMFCs perform slightly better after the break-in fuel is replaced. The re-introduction of nitrogen sparging shortly after the fuel replacement resulted in no improvement, indicating that the nitrogen sparging itself is not the source of the improvement.

4. Conclusion

After a series of thorough investigations, it is apparent that the application of pressure to the anode fuel loop of a direct methanol fuel cell results in a premature current density limitation most likely resulting from increased mass-transfer limitations at the anode. The application of pressure is found to produce consistent changes in cell behavior and does not appear to damage cell components.

When vacuum is applied, enhancement of cell performance is observed. This enhancement is found to be inherently different from, and may be seen in addition to, pressure gradient increases across the membrane electrode assembly for the purposes of preventing methanol crossover.

Pressure was found to be closely related to current density, with little effect after the limit of CO₂ solubility is reached. That liquid–liquid binary diffusion coefficients are independent of pressure is a strong indication that the pressure applied did not affect the diffusion of liquid methanol to the catalyst surface. With changes to the flow-rate of oxygen at the cathode having no effect under the prescribed conditions, process of elimination suggests that the increase in carbon dioxide concentration in the liquid phase is responsible for the observed performance changes. The mechanism by which this occurs is unknown, though a plausible explanation is that a concentration gradient induced mass transport limitation prevents desorption of carbon dioxide from the catalyst surface. Nijhuis et al. [12] make the claim that the rate of CO₂ desorption must be considered in the platinum catalyzed oxidation of carbon monoxide based on evidence that CO₂ is produced from adsorbed carbon monoxide and oxygen on the catalyst by an equilibrium reaction that is faster than the CO₂ desorption. The extent to which this is directly applicable in a DMFC anode reaction with a Pt–Ru catalyst is admittedly questionable, since the precise reaction mechanism of methanol on a Pt–Ru catalyst remains a matter of debate [13].

While there is substantial evidence that CO₂ plays a role in the limiting current density at high pressure, there is equally substantial evidence that the mass transfer rate of methanol to the catalyst surface produces the limiting current density at atmospheric pressure. The two are reconciled by concluding that the adsorption rate of methanol and the desorption rate of CO₂ are both first order processes and that the reaction occurs in a range where changes to the concentration gradient of either will affect the overall rate of reaction. This is in line with the explanation that there is an accumulation of losses that result in the observed cell performance, which the elevated level of CO₂ and decreased level of methanol in solution both contribute to.

The results of the time based study are a confirmation of the assertion that CO₂ is a significant issue regarding cell performance that requires attention. The accumulation of CO₂ in the recycled fuel solution is the primary source of loss in power density. Aside from CO₂, studies have found that only formaldehyde and formic acid are formed in significant quantities, with methylformate and 1,1-dimethoxy methane appearing rarely under specific conditions. The same studies have shown that formaldehyde and formic acid continue to be oxidized to CO₂ as intermediates in a parallel reaction path to that of methanol [15]. Without the formation of a significant poisoning byproduct, CO₂ is the only species likely to be affected by stripping with nitrogen gas. The final conclusion is

that anode fuel recycling is undesirable without a mechanism to remove dissolved carbon dioxide.

Acknowledgement

This work was supported by the United States Army under Agreement No. DAAB07-03-3-K414.

References

- [1] B. Gurau, E.S. Smotkin, *J. Power Sources* 112 (2002) 339–352.
- [2] J. Han, J. Ge, H. Liu, *J. Power Sources* 164 (2007) 90–93.
- [3] Y.H. Cai, J. Hu, H. Ma, B. Yi, H.M. Zhang, *Electrochem. Acta* 51 (2006) 6361–6366.
- [4] M.M. Mench, S. Boslet, S. Thynell, J. Scott, *Proceedings of the Symposium on Direct Methanol Fuel Cells. The 199th Electrochem. Soc. Proc. Series*, 2001.
- [5] Argyropoulos, K. Scott, W.M. Taama, *J. Appl. Electrochem.* 31 (2001) 823–832.
- [6] H. Yang, T. Zaho, Q. Ye, *J. Power Sources* 139 (2005) 79–90.
- [7] M.D. Lundin, M.J. McCready, *J. Power Sources* 172 (2007) 553–559.
- [8] P.P. Schonewill, *Oscillatory flow: effect on transverse diffusivity and inertial migration of particles and bubbles*, Ph.D. Thesis, University of Notre Dame du lac, 2008.
- [9] R. Reid, J. Prausnitz, B. Poling, *The Properties of Liquids and Gases*, fourth edition, McGraw-Hill Book Company, 1987.
- [10] R.J. Bellows, E.P. Marucchi-Soos, D.T. Buckley, *Ind. Eng. Chem. Res.* 35 (1996) 1235–1242.
- [11] J. Carroll, J. Slupsky, A. Mather, *J. Phys. Chem. Ref. Data* 20 (1991) 1201–1209.
- [12] T. Nijhuis, M. Makkee, A.D. van Langeveld, J.A. Moulijn, *Appl. Catal. A: Gen.* 164 (1997) 237–249.
- [13] C. Lamy, E.M. Belgsir, J.M. Leger, *J. Appl. Electrochem.* 31 (2001) 799–809.
- [15] H. Wang, C. Wingender, H. Baltruschat, M. Lopez, M. Reetz, *J. Electroanal. Chem.* 509 (2001) 163–169.